EClinicalMedicine 34 (2021) 100778

Contents lists available at ScienceDirect

EClinicalMedicine

journal homepage: https://www.journals.elsevier.com/eclinicalmedicine

Research Paper

Assessment of pulmonary arterial circulation 3 months after hospitalization for SARS-CoV-2 pneumonia: Dual-energy CT (DECT) angiographic study in 55 patients

Martine Remy-Jardin[a,b,*], Louise Duthoit[b,c], Thierry Perez[b,d], Paul Felloni[a,b], Jean-Baptiste Faivre[a,b], Stéphanie Fry[b,c], Nathalie Bautin[b,c], Cécile Chenivesse[b,c], Jacques Remy[a,b], Alain Duhamel[e]

[a] Univ.Lille, CHU Lille, Department of Thoracic Imaging, ULR 2694 METRICS Evaluation des technologies de santé et des pratiques médicales, F-59000 LILLE, France
[b] Hospital Calmette, University Hospital Center of Lille, Blvd Jules Leclercq F-59000 LILLE, France
[c] Univ.Lille, CHU Lille, Department of Pulmonology, Hospital Calmette, University Hospital Center of Lille, Blvd Jules Leclercq, F-59000 LILLE, France
[d] Department of Pulmonary Function Testing, Hospital Calmette, University Hospital Center of Lille, Blvd Jules Leclercq, F-59000 LILLE, France
[e] Univ.Lille, CHU Lille, Department of Biostatistics, ULR 2694 METRICS Evaluation des technologies de santé et des pratiques médicales, F-59000 LILLE, France

ARTICLE INFO

Article History:
Received 3 January 2021
Revised 11 February 2021
Accepted 11 February 2021
Available online xxx

Keywords:
CT angiography
Dual-energy CT
Lung perfusion
Pulmonary embolism
COVID-19

ABSTRACT

Background: During COVID-19, the main manifestations of the disease are not only pneumonia but also coagulation disorders. The purpose of this study was to evaluate pulmonary vascular abnormalities 3 months after hospitalization for SARS-CoV-2 pneumonia in patients with persistent respiratory symptoms.
Methods: Among the 320 patients who participated in a systematic follow-up 3 months after hospitalization, 76 patients had residual symptoms justifying a specialized follow-up in the department of pulmonology. Among them, dual-energy CT angiography (DECTA) was obtained in 55 patients.
Findings: The 55 patients had partial (n = 40; 72.7%) or complete (n = 15; 27.3%) resolution of COVID-19 lung infiltration. DECTA was normal in 52 patients (52/55; 94.6%) and showed endoluminal filling defects in 3 patients (3/55; 5.4%) at the level of one (n = 1) and two (n = 1) segmental arteries of a single lobe and within central and peripheral arteries (n = 1). DECT lung perfusion was rated as non-interpretable (n = 2;3.6%), normal (n = 17; 30.9%) and abnormal (n = 36; 65.5%), the latter group comprising 32 patients with residual COVID-19 opacities (32/36; 89%) and 4 patients with normal lung parenchyma (4/36; 11%). Perfusion abnormalities consisted of (a) patchy defects (30/36; 83%), (b) PE-type defects (6/36; 16.6%) with (n = 1) or without proximal thrombosis (n = 5); and (c) focal areas of hypoperfusion (2/36; 5.5%). Increased perfusion was seen in 15 patients, always matching GGOs, bands and/or vascular tree-in- bud patterns.
Interpretation: DECT depicted proximal arterial thrombosis in 5.4% of patients and perfusion abnormalities suggestive of widespread microangiopathy in 65.5% of patients. Lung microcirculation was abnormal in 4 patients with normal lung parenchyma.

Introduction

Since the onset of the COVID-19 pandemic, the radiological literature has reported the characteristic findings of COVID-19 pneumonia, which most frequently include bilateral, peripheral, often rounded-ground-glass opacities that are predominantly located in the lower lobes, often accompanied by consolidation [1]. During the acute phase of the disease, case reports and autopsy findings rapidly alerted the medical community on coagulation abnormalities, raising questions on whether thrombotic and embolic events worsened the patient's clinical status [2–6]. This led to modify the indications for chest CT in COVID-19 patients, primarily limited to non-contrast examinations for the evaluation of parenchymal abnormalities or assessment of alternative diagnoses. CT angiography was then considered in the management of patients exhibiting acute or subacute respiratory distress, enabling depiction of endoluminal filling defects in up to 30% of patients, mainly located within segmental and subsegmental arteries [7–12]. Although endoluminal clots could result from a thromboembolic disease, autopsy studies highlighted changes consistent with thrombosis occurring within the pulmonary arterial circulation in the absence of apparent embolism [5]. This was also

Funding: No funding was received for this study.
* Corresponding author.
E-mail address: martine.remy@chru-lille.fr (M. Remy-Jardin).

https://doi.org/10.1016/j.eclinm.2021.100778

Research in context

Evidence before this study

During COVID-19, the main manifestations of the disease are not only pneumonia but also coagulation disorders. Based on literature review that included CT angiographic examinations, endoluminal filling defects were detected in up to 30% of patients, mainly located within segmental and subsegmental arteries. Although endoluminal clots could result from a thromboembolic disease, autopsy studies highlighted changes consistent with thrombosis occurring within the pulmonary arterial circulation in the absence of apparent embolism. This was also clinically suggested by the low proportion of patients with PE in whom deep vein thrombosis was diagnosed.

The second aspect of the COVID-19 vasculopathy lies at the level of lung microcirculation. Autopsy studies highlighted the severe endothelial injury associated with intracellular virus and disrupted cell membranes with widespread capillary microthrombi. Patients with COVID-19 also exhibited a high amount of new vessel growth

When CT angiography was obtained with dual-energy (DE), standard CT angiographic images were completed by lung perfusion images enabling analysis of lung microcirculation. In the early clinical phase, increased lung perfusion matching with ground-glass opacities was reported. At a later phase of the disease, widespread perfusion defects were described in a majority of patients as well as halos of increased perfusion surrounding hypoperfused areas of consolidation, the latter suggesting the detectability of microvascular changes within areas of COVID-19 pneumonia.

Added value of this study

This is the first study reporting pulmonary circulation status in the follow-up of COVID-19 survivors remaining symptomatic 3 months after hospitalization for a severe SARS-CoV-2 pneumonia.

Dual-energy CT (DECT) angiography depicted unexpected proximal arterial thrombosis in 5.4% of patients

DECT lung perfusion abnormalities suggestive of widespread microangiopathy were identified in 65.5% of patients.

In addition to perfusion defects, perfusion imaging also allowed depiction of areas increased perfusion matching residual SARS-CoV-2 pneumonia abnormalities.

Implications of all the available evidence

This study suggests the presence of multiple residual changes within central and peripheral pulmonary circulation in the months following COVID-19 pneumonia that can help understand patient functional complaint. It also highlights the persistent risk for pulmonary artery thrombosis.

clinically suggested by the low proportion of patients with PE in whom deep vein thrombosis was diagnosed [8,9].

The second aspect of the COVID-19 vasculopathy lies at the level of lung microcirculation. Autopsy studies highlighted the severe endothelial injury associated with intracellular virus and disrupted cell membranes with widespread capillary microthrombi [13,14]. In comparison with autopsy findings in influenza-associated respiratory failure, alveolar capillary microthrombi were found to be 9 times more prevalent in patients with COVID-19 who also exhibited a 2.7 times higher amount of new vessel growth [13]. In-vivo insight into this distal pulmonary angiopathy was reported in patients with mild to severe COVID-19 pneumonia who underwent dual-energy CT angiography [15–20]. In the early clinical phase, increased lung perfusion matching with ground-glass opacities was reported. At a later phase of the disease, widespread perfusion defects were described in a majority of patients as well as halos of increased perfusion surrounding hypoperfused areas of consolidation, the latter suggesting the detectability of microvascular changes within areas of COVID-19 pneumonia. Complex interactions between ventilation and perfusion are also to be considered. A mathematical model has recently raised hypotheses on the combined effects of pulmonary embolism, ventilation-perfusion mismatching in the non-injured lung and normal perfusion of the relatively small fraction of injured lung to explain early COVID-19 hypoxemia [21]. Although the long-term outcome of vascular changes is still unknown, the state of perfusion of lung tissue at the different phases of COVID-19 pneumonia appears to be an important parameter for a proper understanding of physiological derangements [22].

The primary objective of the present study was to investigate the morphologic and perfusion changes within pulmonary circulation three months after hospitalization for COVID-19 pneumonia in a cohort of 55 patients with persistent respiratory symptoms who underwent dual-energy (DE) CT angiography. The secondary objective was to search for differences in patient characteristics according to the results of DECT perfusion imaging.

Materials & methods

Study population

All patients who had been hospitalized for COVID-19 pneumonia confirmed by RT-PCR analysis of throat specimens between March and April 2020 in our center were offered a systematic follow-up at 3 months by the Department of Infectious Diseases. The criteria for hospitalization included the presence of dyspnea, a respiratory rate of 30 or more breaths per minute, a blood oxygen saturation of 93% or less, a ratio of the partial pressure of arterial oxygen to the fraction of inspired oxygen ($Pa02:FiO_2$) of less than 300 mm Hg and/or infiltrates in more than 50% of the lung field. There were two broad categories of hospitalized patients: (a) patients with a critical respiratory status, justifying to be admitted in the ICU; and (b) patients in less severe conditions, requiring management in a non-ICU department.

At the time of follow-up (**Fig. 1**), 76 patients presenting with residual respiratory symptoms (i.e., dyspnea, dry cough) and/or concern on chest radiographic abnormalities were referred to the Department of Pulmonology for specialized follow-up. The pulmonologists in charge of COVID-19 follow-up considered that 9 patients did not require further evaluation as their residual symptoms and/or chest radiographic abnormalities did not differ from those observed before COVID-19, explained by a pre-existing underlying respiratory disease. The clinical presentation of the remaining 67 patients justified further investigation with chest CT angiography (CTA) and pulmonary function tests (PFTs). All patients underwent chest CT that could not be obtained with administration of contrast material due to renal insufficiency in 7 patients. Five patients underwent single-energy CTA in a community center only equipped with this technology and 55 patients underwent a dual-energy CT angiographic study in our department. Because lung perfusion is only available on dual-energy chest CT angiographic examinations, our study population was limited to these 55 patients.

All patients underwent chest CT which consisted of non-contrast examinations (n = 7; renal insufficiency), single-energy (n = 5) and dual-energy (n = 55) (DECT) CT angiographic studies. The subgroup of 55 patients with DECT angiographic follow-up was the study population of this investigation.

PFTs were available in 46 patients (84%) and not performed in 9 patients (16%) (patient refusal: n = 3; equipment not available

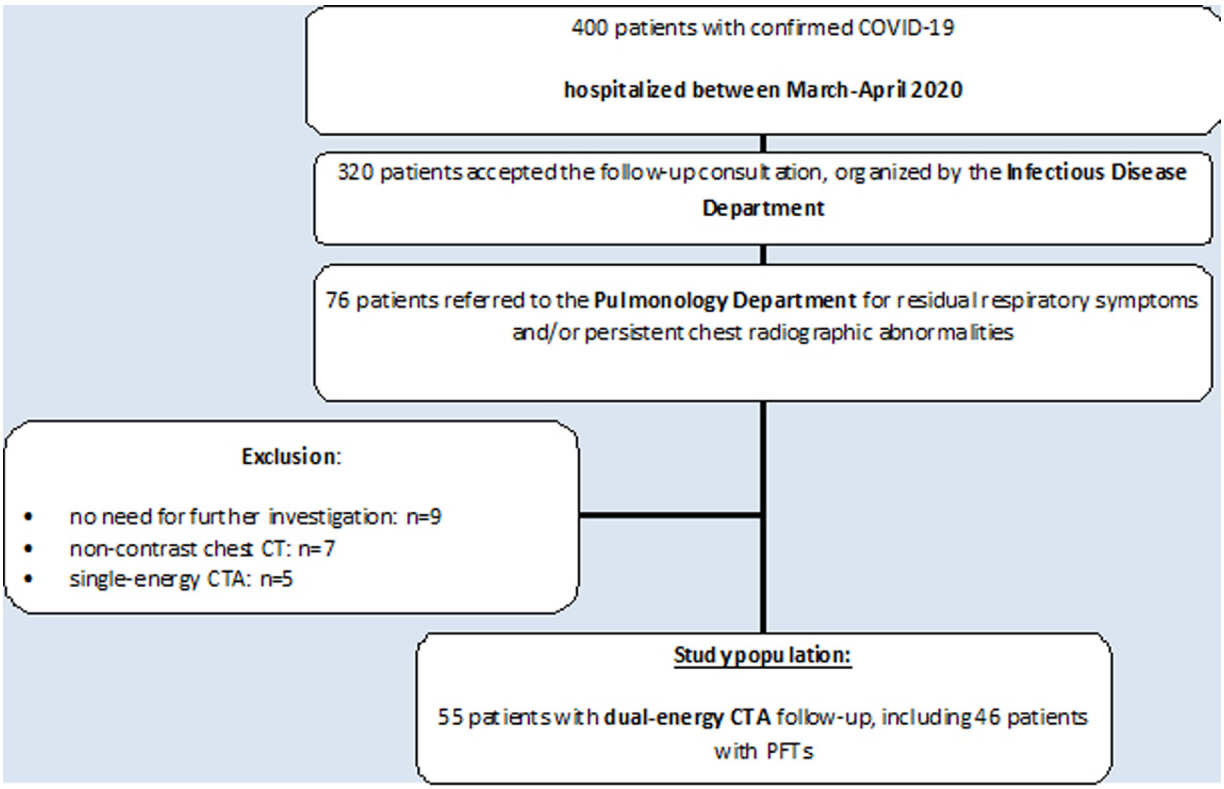

Fig. 1. Flow-chart of the study population.

at the time of CT examination: n = 6). The study population included consecutive patients requiring follow-up with retrospective analysis of data. All data used in this study were retrieved from patient files (clinical, biological, functional and therapeutic data); CT images were accessible via the PACS system; all data were available for clinical research purposes. This retrospective, non-interventional observational study was approved by the local Ethics Committee (Comité de Protection des Personnes Nord Ouest IV, registered in the Office for Human Research Protection Database IORG 0,009,553) with vaiwer of patient informed consent according to national and European regulatory rules and general data protection regulation (GDPR). This study was conducted in agreement with the French law of August 9, 2004, completed by the law n° 2012–300 of March 5, 2012. No industrial support was given to the authors.

Study aims and endpoints

The aim of the study was to investigate the morphologic and perfusion changes within pulmonary circulation three months after hospitalization for COVID-19 pneumonia in a cohort of 55 patients with persistent respiratory symptoms who underwent dual-energy (DE) CT angiography. The primary endpoint was to analyze the presence of endoluminal clots within pulmonary arteries and abnormalities of lung microcirculation on DECT iodine maps. Because DECT lung perfusion cannot be interpreted without precise knowledge of lung parenchymal status, this investigation also included the analysis of corresponding lung images with special evaluation of residual abnormalities of the COVID-19 pneumonia and potential presence of comorbid conditions such as emphysema and interstitial lung disease. Secondary endpoints investigated whether differences in patient characteristics could be observed according to the results of DECT perfusion imaging.

Imaging evaluation

CT protocol

The study population underwent a dual-energy CT angiographic (CTA) examination on a 3rd-generation dual-source CT system (Somatom Force, Siemens Healthineers, Forchheim, Germany) with injection of 60 – 90 mL of a 40% iodinated contrast material at a rate of 3–4 mL/*sec*. From each data set, three series of images were generated: (a) contiguous, 1 mm thick lung and mediastinal images, reconstructed with high resolution and soft kernels (Bl 57 and Br 36, respectively); and 1-mm thick lung perfusion images using the Lung PBV software (Siemens Healthineers, Forchheim, Germany).This was completed by a second set of perfusion images, generated by subtraction of low- and high-monoenergetic images, to generate less noisy images in this population mainly composed of overweight and obese patients. This was obtained on the eXamine prototype (Siemens Healthineers, Forchheim, Germany).

The percentage of COVID-19 lung infiltration, further referred to as the “CT COVID score” was calculated using an AI-software prototype (CT Pneumonia Analysis; Siemens Healthineers, Forchheim, Germany). The algorithm uses CT data to automatically identify and 3D-segment both the lung parenchyma and abnormal areas of ground-glass opacities and consolidation. The software outputs a percentage of total lung involvement (by both GGO and consolidation) [23]. Follow-up chest CTA was systematically completed by a volumetric, non-contrast, single-energy acquisition at expiration to detect air trapping, i.e., a potential confounder for perfusion defect interpretation.

Evaluation of lung and mediastinal images and lung perfusion images

Pulmonary arterial circulation was analyzed on mediastinal and perfusion images. On mediastinal images, we searched for the presence of endoluminal filling defects from central to subsegmental arterial divisions. On perfusion images, we rated the presence of: (a)

perfusion defects of 3 types: patchy defects, PE-type defects and non-systematized areas of hypoperfusion; and (b) areas of increased perfusion. The iodine concentration, expressed in mg of iodine per mL of lung volume, was calculated for both lungs.

On lung images, we recorded the presence and extent of post COVID-19 abnormalities, including ground-glass opacities, bands, consolidation and features of fibrosis (i.e., honeycomb cysts) or features potentially suggestive of fibrosis (i.e., bronchial and/or bronchiolar dilatation within areas of ground-glass opacities and/or reticulation). Their distribution was rated as unilateral/bilateral; central/peripheral. We also searched for the presence of vascular features described in the acute phase of COVID-19 pneumonia, i.e., the "vascular tree-in-bud" pattern and abnormally dilated peripheral vessels [17]. The presence, extent and severity of comorbid conditions that might interfere with CT lung perfusion analysis, i.e., emphysema and interstitial lung disease, was also recorded. Emphysema was rated as mild when limited to centrilobular emphysema, moderate when lung destruction was more pronounced but without reaching the level of panlobular emphysema, and severe in presence of panlobular emphysema. The extent of emphysema was rated as limited when involving exclusively the upper lobes, and diffuse when observed from to bottom of the lungs. ILD was rated as fibrosing or non-fibrosing, and limited (<10% of the lung volume) or diffuse in distribution. Air trapping was searched for on expiratory scans.

Pulmonary function evaluation

Pulmonary function tests included a spirometry with forced vital capacity (FVC) and slow vital capacity (VC), plethysmographic lung volumes and a single-breath DLCO according to ATS/ERS guidelines and the 1993 ERS predicted values were used [24,25]. The list of PFT parameters comprised vital capacity, forced vital capacity, forced expiratory volume in one second, forced residual capacity, residual volume, total lung capacity, diffusing capacity of the lung for carbon monoxide and alveolar capillary blood volume.

Study aims and endpoints

The primary objective of this study was to investigate the morphologic and perfusion changes within pulmonary circulation three months after hospitalization for COVID-19 pneumonia. The endpoints for the primary objective were the presence of endoluminal filling defects within central and peripheral pulmonary arteries on morphologic images and the presence of perfusion abnormalities, including perfusion defects and areas of increased perfusion, on perfusion images. On lung images, we searched for CT features suggestive of residual COVID-19 lung infiltration and the presence of any co-morbid conditions, unrelated to COVID-10 sequellae, that could alter lung perfusion.

The secondary objective was to search for differences in patients'characteristics according to the results of DECT perfusion images. The endpoints for this secondary objective concerned the patients' status at the time of the early phase of COVID-19 pneumonia, the pulmonary function profile, the quantitiative analysis of the iodine content on perfusion images.

Condition of image analysis

The reading of morphologic and perfusion imaging was obtained by consensus between two senior chest radiologists with 7 and 14 years of experience in DECT lung perfusion analysis, respectively. A separate analysis of lung, mediastinal and perfusion images, presented in random order, was first undertaken. A second reading session was organized with a combined reading of lung and perfusion images of each patient to superimpose perfusion abnormalities on the corresponding morphological background.

Statistical analysis

Categorical variables are expressed as number and percentages. Continuous variables were reported as means and standard deviations (SD) in the case of normal distribution or medians (interquartile, IQR) otherwise. Normality of distributions was assessed using histograms and the Shapiro-Wilk test. Comparisons of clinical data and PFTs between patients with normal and abnormal lung perfusion were performed with the Mann-Whitney test for quantitative variables and the chi-square test (or Fisher exact test) for categorical variables. The condition of validity of the chi-square test (all expected values greater or equal to 5) was checked. We did not perform comparisons when a group included less than 10 patients. Statistical testing was conducted at the two-tailed α-level of 0.05 and was considered as an exploratory analysis. Data were analyzed using the SAS software version 9.4 (SAS Institute Inc, Cary, NC 25,513).

Role of funding

No funding was received for this work

Results

Characteristics of the study population

As shown in **Table 1**, the study population of 55 patients (42 males; 13 females; mean age: 59.7 year) included 24 smokers (43.6%) and 11 patients (20.0%) had respiratory comorbidities. The median BMI was 27.1 kg/m^2; the study group was mainly composed of overweight (n = 21; 38.2%) and obese (n = 19; 34.5%).

Table 2 summarizes the clinical and biological data of the study population at the time of COVID-19 lung infection: (a) 23 patients (41.8%) had been admitted to the ICU; (b) COVID-19 imaging was obtained by chest X-ray alone in 20 patients (36.3%) and completed by chest CT in 35 patients (63.7%) with a mean ($\pm$ SD) score of COVID-19 lung abnormalities of 34.0% ($\pm$ 23.7); (c) acute PE was diagnosed in the absence of major predisposing factors in 5 patients (9.1%); (d) 36 patients (65.5%) received prophylactic anticoagulation. The standard of care proposed in our institution at the time of early COVID-19 pandemic included the following therapeutic options, i.e., probabilistic antibiotherapy, systemic corticotherapy and/or anticoagulation while antiviral therapy was only administered to patients who accepted to be enrolled in the European DISCOVERY trial. Details for our study population is given in **Table 2**.

The median (interquartile range) interval of time between COVID-19 and follow-up CTA was 144.0 (Q1; Q3: 121.0; 157.0) days. Forty-six patients underwent PFTs within 8 days after CTA. Functional parameters are summarized in **Table 3**. The mean ($\pm$SD) DLCO was 78.6 $\pm$ 16.1%.

Lung parenchymal findings

COVID-19 residual findings were identified in 40 patients (72.7%) whereas 15 patients (27.3%) had normal chest CT. Lung abnormalities included areas of ground-glass attenuation (39/40), alone or superimposed on fine linear opacities, and parenchymal bands (21/40). Seven patients (7/40) showed bronchial/bronchiolar dilatation within areas of ground-glass attenuation, seen in association with fine reticulation, suggestive of a potential evolution towards lung fibrosis; there was no feature of honeycombing. Lung abnormalities were mostly bilateral (36/40), with a diffuse distribution in all but 4 patients showing a predominant distribution in the peripheral lung zones (n = 4). One patient showed subtle "vascular tree-in-bud" pattern in peripheral lung zones of both lungs. Abnormally dilated peripheral vessels were not identified. The median CT score of post COVID-19 lung infiltration was 0.85% (Q1; Q3: 0.32; 2.52). In the 35 patients

Table 1
Characteristics of the study population at the time of COVID 19 follow-up (n = 55).

Variable	Results
Males, n (%) /**females**, n (%)	42 (76.4%) −13 (23.6%)
Age, year	
mean ± SD	59.7 ± 13.7
range	27.1 to 83.6
Smokers, n (%)	24 (43.6%)
Tobacco consumption, pack-year	
median (Q1; Q3)	20.0 (8.5; 30)
range	1 to 75
Respiratory co-morbidities, n (%)	11 (20%)
- COPD, n	3
- asthma, n	4
- interstitial lung disease, n	3
- peripheral lung carcinoma, n	1
Patient medical history, n (%)	23 (42%)
- chronic kidney disease, n	1
- cardiovascular disease, n	11
- type 2 diabetes, n	9
- hypertension, n	22
- extra-thoracic tumor, n	0
Body-mass-index (BMI), kg/m^2	
median (Q1; Q3)	27.1 (24.6; 32.4)
range	19.9 to 41.4
Body-mass-index (BMI) categories,	
- <18.5 kg/m^2(*underweight patient*), n (%)	0
- 18.5 -<25 kg/m^2(*normal BMI*), n (%)	15 (27.3)
- 25 −30 kg/m^2 (*overweight patient*), n (%)	21 (38.2)
- >30 kg/m^2 (*obese patient*), n (%)	19 (34.5)

Abbreviations: yr: year; COPD: chronic obstructive pulmonary disease; SD: standard deviation; Q1: 1st quartile; Q3: 3rd quartile.

Table 2
Characteristics of the study population at first hospital admission (n = 55).

Variable	Results
Clinical data	
-admission to the ICU, n (%)	23 (41.8%)
-mechanical ventilation, n (%)	16 (29.0%)
-COVID-19 imaging by chest X-ray alone, n (%)	20 (36.3%)
-COVID-19 imaging by chest X-ray and CT, n (%)	35 (63.7%)
-CT score of COVID-19 lung abnormalities,%	34.0 ± 23.7
mean (± SD)	31.9
median	15.7; 55.0
Q1; Q3	5 (9%)
-diagnosis of acute pulmonary embolism, n (%)	0
-previous history of thrombo-embolic disease, n (%)	36 (65.4%)
-prophylactic anticoagulation, n (%)	
Biological data	
-C-reactive protein (7 missing)	88.0 (42.0; 115.0)
median (Q1; Q3)	14.0 to 347.0
range	0.35 (0.23; 0.50
-Urea nitrogen	0.14 to 1.4
median (Q1; Q3)	8.0 (7.0; 11.0)
range	5.0 to 60.0
-Creatinine	43.0 (31.0; 63.0)
median (Q1; Q3)	13.0 to 307.0
range	31.0 (21.0; 51.0)
-ASAT	8.0 to 237.0
median (Q1; Q3)	373.0 (313.0; 482.0)
range	144.0 to 1465.0
-ALAT	12.9 ± 1.9
median (Q1; Q3)	7.1 (5.4; 9.3)
range	2.7 to 26.6
-Lactate dehydrogenase (4 missing)	5.4 (3.8; 7.4)
median (Q1; Q3)	1.7 to 24.60
range	6.4 (2.9; 10.6)
-Hemoglobin	1.3 to 82
mean (± SD)	1590.0 (1150.0; 3010.0)
-Leucocytes	330.0 to 4000.0
median (Q1; Q3)	
range	
-Neurophils (3 missing)	
median (Q1; Q3)	
range	
-Neutrophil-to-lymphocyte ratio (3 missing)	
median (Q1; Q3)	
range	
-D-dimers (20 missing)	
median (Q1; Q3)	
range	
Therapeutic measures	
-probabilistic antibiotherapy, n	40 (72.7%)
-systemic corticotherapy, n	12 (21.8%)
-anticoagulation, n	41 (74.5%)
-antiviral therapy, n	15 (27.3%)

Abbreviations: ICU: intensive care unit; SD: standard deviation; Q1: 1st quartile; Q3: 3rd quartile.

with chest CT obtained at the acute phase of the disease: (a) the median COVID CT score was 31.9% (Q1: 15.7; Q3: 55.8); (b) the median difference of COVID CT scores was 28.3% (Q1: 11.5; Q3: 53.7).

Emphysema was identified in 10 patients (severe: n = 1; moderate: n = 2; mild: n = 7), diffusely distributed in 3 patients and exclusively seen in the upper lobes in 7 patients. Two patients had CT features of basal and peripheral fibrosing ILD involving <10% of lung volume.

CT angiographic findings

In 3 patients (3/55; 5.4%), endoluminal filling defects were identified at the level of: (a) one (n = 1) and two (n = 1) segmental pulmonary arteries of a single lobe; these filling defects were non-obstructive; and (b) central and peripheral pulmonary arteries of both lungs (n = 1); they consisted of multiple obstructive and non-obstructive endoluminal filling defects. Lung parenchymal images of the 3 patients showed residual COVID-19 lung abnormalities, mostly represented by disseminated ground glass attenuation and a few basal bands; there were no CT features of recent lung infarction. Following CT angiography, Doppler ultrasonographic examination was obtained; none of these patients had deep venous thrombosis. At the time of acute viral infection: (a) none of these patients had pulmonary artery thrombosis;(b) they did not receive preventive anticoagulation during the hospitalization.

Lung perfusion findings

Descriptive analysis of perfusion images

Perfusion images were (a) non-interpretable in 2/55 patients (3.6%), owing to marked artifacts in the context of morbid obesity and/or shoulder prosthetic material; (b) normal in 17 patients (30.9%); and (c) abnormal in 36 patients (65.5%).

Perfusion abnormalities consisted of a variable association of: (a) patchy perfusion defects (30/36; 83%), seen as disseminated abnormalities;(b) PE-type perfusion defects (6/36; 16.6%) in presence (n = 1) or absence of proximal thrombosis (n = 5); multiple segmental and subsegmental defects were seen in both lungs in the patient with multiple endoluminal clots (Fig. 2); a few (1−5 defects/patient), peripheral and small-sized (<subsegmental size) defects were seen in the 5 patients without endoluminal clots; and (c) focal areas of non-systematized hypoperfusion (2/36; 5.5%). In 15 patients with perfusion defects (15/36; 41.6%), focal areas of increased perfusion were also depicted.

Combined reading of perfusion and lung images

When lung perfusion was rated as abnormal (n = 36), corresponding lung images showed residual COVID-19 opacities in 32 patients (32/36; 89%) and normal lung parenchyma in 4 patients (4/36; 11%).

Table 3
Pulmonary function tests in the study population (n = 46).

VC,% pred	
mean ± SD	102.0 ± 20.4
range	71.6 to 155.3
FVC,% pred	
mean ± SD	102.0 ± 19.8
range	68.04 to 155.0
FEV1/FVC	
mean ± SD	0.78 ± 0.09
range	0.43 to 0.93
FRC,% pred	
mean ± SD	100.3 ± 20.9
range	62.1 to 156.7
RV,% pred	
mean ± SD	97.2 ± 23.3
range	55.2 to 165.5
TLC,% pred	
mean ± SD	94.8 ± 14.1
range	67.2 to 131.4
DLCO,% pred	
mean ± SD	78.6 ± 16.1
range	46.9 to 112.4
DLCO/VA,% pred	
mean ± SD	94.8 ± 15.7
range	56.3 to 130.1

Abbreviations: VC: vital capacity; FVC: forced vital capacity; FEV1: forced expiratory volume in one second; FRC: forced residual capacity; RV: residual volume; TLC: total lung capacity; DLCO: diffusing capacity of the lung for carbon monoxide; VA: alveolar capillary blood volume.
SD: standard deviation; Q1: 1st quartile; Q3: 3rd quartile.
NB: Results are expressed with an accuracy of 2 decimal places when values are less than 1.

When PE-type defects were identified in the absence of endoluminal clots (n = 5), lung images showed: (a) no features of COVID-19 in 3 patients (Fig. 3); (b) features suggestive of peripheral chronic PE in corresponding areas in 2 patients (Fig. 4); (c) the absence of bronchiolectasis, emphysema and/or air trapping at the level of corresponding areas.

When areas of increased perfusion were depicted (n = 15), they were superimposed on (a) ground-glass opacities or parenchymal bands in 14 patients (Fig. 5; Fig. 6); (b) vascular tree-in-bud opacities in the only patient showing this lung abnormality (Fig. 7). Ten of these patients (10/15; 67%) had been admitted to the ICU.

In the 4 patients with normal lung images, abnormal perfusion consisted of patchy defects.

Comparison of patients with normal and abnormal perfusion

Compared with patients with normal perfusion (Table 4), patients with abnormal perfusion:(a) had no significant difference in BMI (p = 0.94) and number of smokers (p = 0.11); (b) had a significantly higher frequency of residual COVID-19 lung infiltration (88.9% versus 35.3%; $p < 0.001$) with no significant difference in the frequency of emphysema (p = 0.14); (c) had been more frequently hospitalized in the ICU (53.8% versus 5.9%; $p<0.001$) and intubated (38.9% versus 5.9%; p = 0.02).The 5 patients with acute PE at the time of admission were all seen with abnormal perfusion on the follow-up DECT examination.

There was no significant difference in the iodine concentration between the 17 patients with normal perfusion and the 36 patients with abnormal perfusion (p = 0.59) (**Table 4**). Median iodine concentration was 1.2 in the 32 patients with abnormal perfusion and 1.4 in the 4 patients with abnormal perfusion in the absence of COVID-19 lung infiltration; no statistical test was performed. As shown in **Table 5**, there was no statistically significant difference in PFT parameters between patients with normal and abnormal perfusion apart from a significantly higher FRC in patients with normal perfusion (median: 107.4 versus 96.6; p = 0.04).

Discussion

To our knowledge, this is the first study describing features within the pulmonary arterial circulation in the follow-up of patients remaining symptomatic 3 months after hospitalization for SARS-CoV-2 infection. At the time of CT follow-up, all patients had a dramatic resolution of the radiologic features of COVID-19 pneumonia with complete clearance in 27.3% of patients and residual

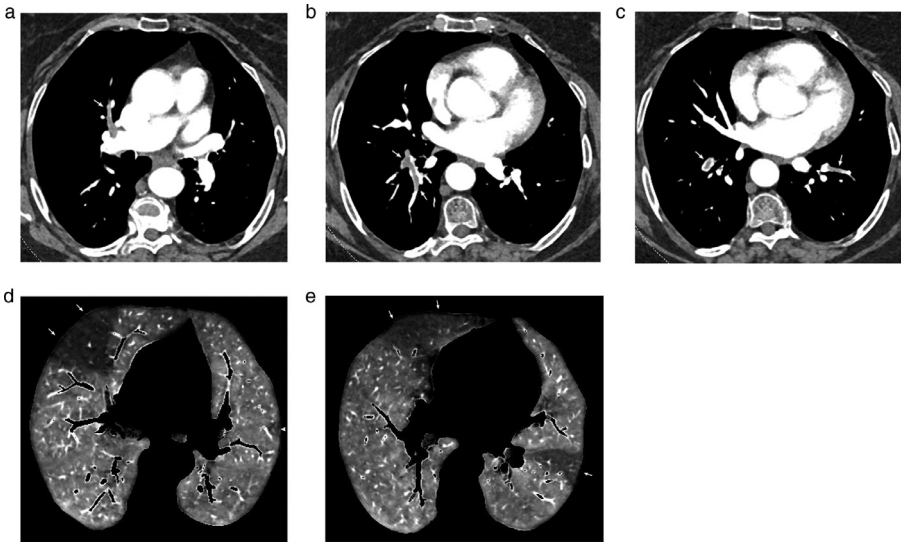

Fig. 2. Dual-energy CT angiography obtained in a 74 yr-old obese female *(BMI: 38.64 kg/m^2)*, **16 weeks after COVID-19 pneumonia with oxygen requirement.**
Mediastinal images obtained at the level of the right bronchus intermedius (**Fig. 2a**) and left atrium (**Fig. 2b-Fig. 2c**) showing multiple filling defects within lobar, segmental and sub-segmental arteries (arrows) in both lungs.
Perfusion images obtained at the level of the upper (**Fig. 2d**) and lower (**Fig. 2e**) lobes showing large PE-type perfusion defects in both lungs (arrows) and a small PE-type defect in the let upper lobe (arrowhead, Fig. 2d).

Fig. 3. Dual-energy CT angiography obtained in a 57 yr-old obese female *(BMI: 33.58 kg/m^2)*, **14 weeks after COVID-19 pneumonia with high-flow oxygen requirement.**

Lung images obtained at the level of the carina (**Fig. 3a**) and right bronchus intermedius (**Fig. 3b**) showing the absence of lung abnormality, in particular at the level of the apical segment of the left lower lobe.

3c: Perfusion image obtained at the same level as that of Fig. 3a showing a peripheral PE-type defect in the apical segment of the left lower lobe (arrows).

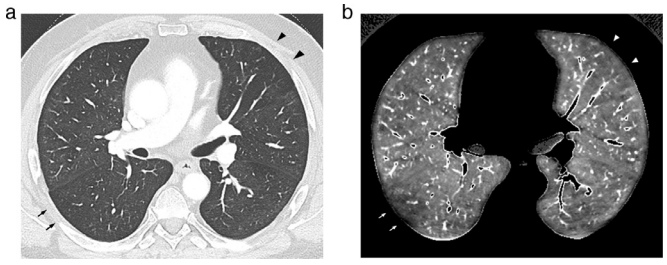

Fig. 4. Dual-energy CT angiography obtained in a 63 yr-old obese male *(BMI: 31.9 kg/m^2)*, **12 weeks after COVID-19 pneumonia requiring invasive ventilation.**

4a**:** Lung image obtained at the level of the right bronchus intermedius showing a triangular zone of hypo-attenuation with small-sized pulmonary vessels suggestive of chronic pulmonary arterial obstruction in the anterior segment of the left upper lobe (arrowheads). Subtle hypoattenuated area in the apical segment of the right lower lobe (arrows).

4b**:** Perfusion image obtained at the same level as that of Fig. 4a showing a PE-type defect in the anterior segment of the left upper lobe (arrowheads) and a peripheral, truncated PE-type defect (arrows) in the apical segment of the right lower lobe.

abnormalities in 72.7% of patients. In the latter group, lung parenchymal abnormalities consisted of ground-glass opacities, mostly of mild attenuation and diffusely distributed, that were seen in isolation or superimposed with fine reticulation. At the time of this early follow-up, evolution toward lung fibrosis was suspected in 7 patients showing bronchial/bronchiolar dilatation within areas of ground-glass attenuation requiring further evaluation before assessing the presence of irreversible fibrotic changes. None of our patients had CT features of honeycombing as described during the acute phase of COVID-19 [26,27].

In this background of post COVID-19 lung changes, CT angiography revealed the presence of endoluminal filling defects in 3 patients (5.4% of the study population). In one patient, there were bilateral

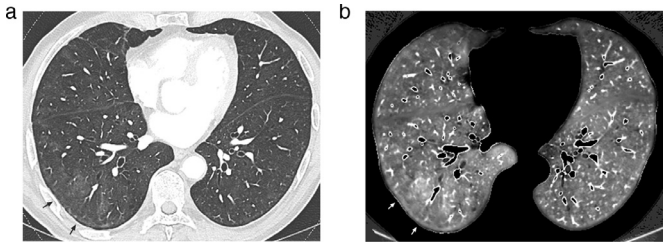

Fig. 5. Dual-energy CT angiography obtained in a 75 yr-old male with normal BMI *(BMI: 23.43 kg/m^2)*, **14 weeks after COVID-19 pneumonia with oxygen requirement.**

5a**:** Lung image obtained at the level of the lower lung zones showing areas of mild ground glass attenuation in the right middle and right lower lobes. The arrows point to the largest area of GGO.

5b**:** Perfusion image obtained at the same level as that of Fig. 5a showing increased perfusion matching with areas of GGO, well demonstrated at the level of the largest area of GGO (arrows).

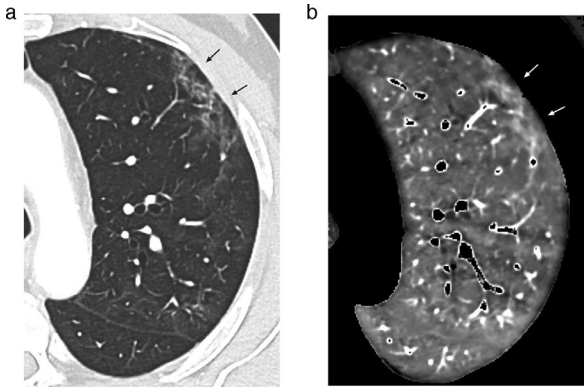

Fig. 6. Dual-energy CT angiography obtained in a 68 yr-old male with normal BMI *(BMI: 24.08 kg/m^2)*, **12 weeks after COVID-19 pneumonia requiring invasive ventilation.**

6a**:** Lung image (magnified view) obtained at the level of the left upper lobe showing dense ground-glass opacities in the peripheral lung (arrows).

6b**:** Perfusion image obtained at the same level as that of Fig. 6a showing increased perfusion matching with peripheral areas of ground-glass attenuation (arrows).

filling defects in central and peripheral pulmonary arteries whereas they were seen in one or two segmental arteries of a single lobe in the remaining 2 patients. These findings were not clinically suspected and lower-limb ultrasound compression obtained immediately after chest CTA did not reveal venous thrombosis. Whereas one cannot categorically exclude thromboembolic disease, the absence of deep

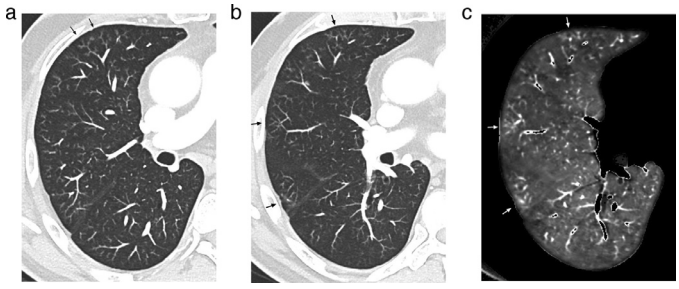

Fig. 7. Dual-energy CT angiography obtained in a 60 yr-old male with normal BMI *(BMI: 24.5 kg/m^2)*, **16 weeks after COVID-19 pneumonia requiring invasive ventilation.**

7a**:** Lung image (magnified view of the right lung; 1-mm thick) obtained at the level of the right bronchus intermedius showing a subtle vascular tree-in-bud pattern in the right lung, more pronounced in the anterior segment of the right upper lobe (arrows).

Lung image (magnified view of the right lung; 3-mm thick, maximum-intensity projection) (**Fig. 7b**) obtained 1 cm below Fig. 7a and corresponding perfusion image (**Fig. 7c**) showing superimposition of areas of increased perfusion on areas of vascular tree-in-bud (arrows).

Table 4
Comparison of clinical and CT characteristics of patients with normal and abnormal perfusion (n = 55).

	Patients with normal lung perfusion (n = 17)	**Patients with abnormal lung perfusion** (n = 36)	**P value**
Body-mass index (BMI), kg/m2			
median (Q1; Q3)	27.1 (24.7; 31.1)	27.4 (24.5; 32.2)	0.94
range	21.9 to 26.5	19.9 to 41.4	
Smokers, n (%)	5 (29.4%)	19 (52.8%)	0.11
Hospitalization in the ICU, n (%)	1 (5.9%)	21 (58.3%)	<0.001
Mechanical ventilation, n (%)	1 (5.9%)	14 (38.9%)	0.02 (*)
Residual COVID-19 lung infiltration, n (%)	6 (35.3%)	32 (88.9%)	<0.001 (*)
Emphysema, n (%)	1 (5.9%)	9 (25%)	0.14 (*)
Iodine concentration, mg iodine/mL			
mean ± SD	1.2 ± 0.4	1.3 ± 0.4	0.59
range	0.32 to 1.8	0.60 to 2.1	

Abbreviations: ICU: intensive care unit; SD: standard deviation; Q1: 1st quartile; Q3: 3rd quartile.
NB: Comparisons were obtained with the Mann-Whitney test for quantitative variables and the chi-square or Fisher exact test (indicated by *) otherwise. P values greater than 0.1 are expressed with 2 decimal places and three decimals otherwise.

venous thrombosis raises the hypothesis of in-situ thrombosis. In keeping with clinical and pathologic descriptions during the acute phase of COVID-19, these findings suggest the possibility of a persistent hypercoagulable state and/or endothelial dysfunction related to the pulmonary microvascular disease described in this study, observed in the weeks following viral pneumonia. It is noticeable that none of these patients had acute PE at the time of COVID-19 and that none received preventive anticoagulation during hospitalization. This high frequency of PE occurring within three months of severe COVID-19 encourages to consider a recent history of COVID-19 as a risk factor for PE and to obtain CT angiographic examinations instead of non-contrast CT scans when these patients are referred for imaging.

Table 5
Comparison of pulmonary function tests between patients with normal and abnormal perfusion (n = 46).

	Patients with normal lung perfusion (n = 14)	**Patients with abnormal lung perfusion** (n = 32)	**P value**
VC,% pred			
median (Q1 ; Q3)	92.9 (87.0; 107.3)	104.8 (85.8; 117.7)	0.25
range	71.6 to 120.0	72.23 to 155.3	
FVC,% pred			
median (Q1 ; Q3)	96.0 (82.6; 110.0)	103.8 (87.9; 117.1)	0.31
range	68.0 to 121.8	72.4 to 155.0	
FEV1/FVC			
median (Q1 ; Q3)	0.82 (0.74; 0.85)	0.80 (0.74; 0.83)	0.41
range	0.43 to 0.91	0.59 to 0.93	
FRC,% pred			
median (Q1 ; Q3)	107.4 (102.1; 115.0)	96.6 (78.1; 114.4)	0.04
range	88.3 to 132.6	62.1 to 156.7	
RV,% pred			
median (Q1 ; Q3)	103.2 (91.9; 120.7)	94.86 (76.0; 110.2)	0.13
range	55.2 to 135.1	60.81 to 165.5	
TLC,% pred			
median (Q1 ; Q3)	93.0 (86.3; 103.1)	95.7 (83.9; 105.0)	0.95
range	79.7 to 117.4	67.2 to 131.4	
DLCO,% pred			
median (Q1 ; Q3)	79.0 (68.0; 86.0)	78.6 (69.0; 89.8)	0.73
range	46.9 to 112.4	51.1 to 109.0	
DLCO/VA,% pred			
median (Q1 ; Q3)	93.0 (87.9; 109.4)	94.4 (82.5; 99.4)	0.96
range	73.4 to 117.1	56.3 to 129.3	

Abbreviations: VC: vital capacity; FVC: forced vital capacity; FEV1: forced expiratory volume in one second; FRC: forced residual capacity; RV: residual volume; TLC: total lung capacity; DLCO: diffusing capacity of the lung for carbon monoxide; VA: alveolar capillary blood volume.
SD: standard deviation; Q1: 1st quartile; Q3: 3rd quartile.
NB: Comparisons were obtained with the Mann-Whitney test. Results are expressed with an accuracy of 2 decimal places when values were less than 1.

Perfusion abnormalities were identified in 36 patients (36/55; 65.5% of the study population). In the absence of knowledge of pulmonary vascular sequelae of COVID-19, one may interpret CT abnormalities in the light of lung microcirculation alterations described during the acute phase of the SARS-CoV-2 infection [13,14]. Disseminated patchy perfusion defects were the most frequent finding, observed in 30 patients (30/36; 83.0%). These abnormalities could represent unresolved/sequelae of the widespread microangiopathy described in the acute phase of the disease, characterized by occlusion of alveolar capillaries. During COVID-19 pneumonia, mottled defects were present in almost all patients scanned with DECT [17,18].

The second finding was the presence of PE-type perfusion defects, depicted in 6 patients (6/36; 16.6%). One patient had multiple, bilateral PE-type defects, explained by obstructive segmental and subsegmental clots in both lungs. In the remaining 5 patients (5/36; 13.8%) who had no detectable clots in the pulmonary arteries, PE-type defects consisted of a few, small-sized peripheral defects. In the absence of previous history of acute thromboembolic event, one may suggest a relationship between these defects and sequelae of thrombi described within pulmonary arteries with a diameter of 1 mm to 2 mm during acute pneumonia, often seen with venous thrombosis. These arterial lesions were often described without complete luminal obstruction [13] which might explain the limited number of these PE-type defects in our study population. During the acute phase of COVID-19 pneumonia, Ildiman et al. reported areas of decreased perfusion without visible thrombus in the lungs of 19% (6 /31) of patients with mild-to-moderate COVID-19, linking these defects to the presence of micro-thrombosis in the lungs (19). Because PE-type defects are nonspecific findings, care was taken to exclude the possibility of false positives in the setting of small-airway disease such as bronchiolectasis, mucous plugging and/or air trapping.

An unexpected finding was the presence of areas of increased perfusion, always seen superimposed on focal areas of ground-glass attenuation or parenchymal bands in 15 patients (15/36; 41.6%). In the early clinical phase of the disease, Si-Mohamed et al. reported diffuse bilateral ground-glass opacities associated with increased lung perfusion in the corresponding lobes in 2 patients [20]. The authors hypothesized that these vascular changes might correspond to the histopathological findings of intussusceptive angiogenesis reported

in autopsy studies, describing the striking neovessels growth in severe COVID-19 pneumonia [13,28]. By analogy, one may suggest the persistence of these microvascular abnormalities on both morphologic and perfusion images [29]. It was interesting to note that areas of increased perfusion also matched the vascular tree-in-bud abnormalities that were observed in a single patient of our cohort who had suffered from an initially severe COVID-19 pneumonia requiring ICU hospitalization. Considering that this pattern was proposed as a potential CT marker of immunothrombosis and angiogenesis in patients with severe COVID-19 pneumonia [13,28], it could be hypothesized that residual lesions remain detectable in the months following COVID-19 pneumonia. Quantification of iodine within both lungs did not show significant differences between the subgroups analyzed. This suggests that perfusion alterations were too subtle for this quantitative analysis on both lungs. As areas of hyperperfusion were always seen in patients with patchy defects, one may also raise the possibility of a compensatory effect of these two types of perfusion abnormalities on the overall quantitative analysis. Pulmonary functional parameters, including diffusing capacity for carbon monoxide, were not found to be significantly different between patients with normal and abnormal perfusion except for FRC. Recent studies have suggested that reduced DLCO and TLC were the main abnormalities observed after COVID-19 [30,31].

This study suffers from several limitations. First, the detection of patchy perfusion defects may have been overestimated in this population mainly composed of large patients. In overweight and obese patients, there is a well-known potential decrease in perfusion image quality due to image graininess directly linked to the patient morphotype. Moreover, it also included smokers but most of them had minor emphysematous changes, limited to the upper lung zones. Second, we did not have pulmonary function tests for all patients, thus precluding the search for correlations between morphology and function. However, one may understand patient reluctance for several investigations after severe lung disease and longstanding hospitalization. Moreover, the PFT facility was not easily available at the time when non-COVID patients needed to be prioritized. Third, perfusion changes were analyzed in the absence of control group, starting with perfusion analysis in normal subjects. However, one can highlight the homogeneity of lung perfusion in nonsmokers that has already been reported in the literature [32,33]. In addition, we did not have comparable control group with viral non-COVID-19 pneumonia. Lastly, the lack of systematic use of DECT at the time of viral pneumonia did not allow comparative analysis of perfusion changes over time. This would have required the availability of dual-energy CT technology in the vicinity of the ICU, only equipped with single-energy CT in our institution.

In conclusion, this study suggests the presence of multiple residual changes within central and peripheral pulmonary circulation in the months following COVID-19 pneumonia that can help understand patient functional complaint. It also highlights the persistent risk for pulmonary artery thrombosis. Long-term follow-up chest imaging of survivors is needed for better understanding of the possible irreversible pulmonary damage of SARS-CoV-2 pneumonia.

Author contribution

MRJ designed the study, participated in data collection, reviewed the data analyses, provided expert analysis for data interpretation, literature search, writing of the manuscript and verification of submitted data. LD, TP participated in the study design, data collection, data analysis and verification of submitted data. PF participated in data collection, data interpretation and verification of submitted data. JBF participated in the study design, data interpretation and verification of submitted data. SF, NB participated in the study design, data collection and verification of submitted data. CC participated in data interpretation, writing of the manuscript and verification of submitted data. JR participated in the literature search and writing of the manuscript. AD participated in data analysis, data interpretation, writing and verification of submitted data. The draft manuscript was written jointly by MRJ, CC and AD and all the authors worked collaboratively to prepare the final content and made the decision to submit the manuscript for publication.

Data sharing statement

For the purpose of reproducing the results or replicating the method, the corresponding author will make the data, analytic methods, and study materials available to other researchers upon request, with investigator support.

Declaration of Competing Interest

Author MRJ received nonfinancial support for clinical research purposes from Siemens Healthineers. Author JR received personal fees as consultant for Siemens Healthineers and non-financial support for clinical research purposes. All other authors have nothing to declare.

Funding

No funding was received for this study.

References

[1] Raptis CA, Hammer MM, Short RG, et al. Chest CT and coronavirus disease (COVID-19): a critical review of the literature to date. AJR 2020;215:1–4.
[2] Connors JM, Levy JH. Thromboinflammation and the hypercoagulability of COVID-19. J Thromb Haemost 2020;18:1559–61.
[3] Han H, Yang L, Liu R, et al. Prominent changes in blood coagulation of patients with SARS-CoV-2 infection. Clin Chem Lab Med 2020;58:1116–20.
[4] Wichmann D, Sperhake JP, Lütgehetmann, et al., et al. Autopsy findings and venous thromboembolism in patients with COVID-19. Ann Intern Med 2020;173:268–77.
[5] Lax SF, Skok K, Zechner P, et al. Pulmonary arterial thrombosis in COVID-19 with fatal outcome: results from a prospective, single-center, clinicopathologic case series. Ann Intern Med 2020;173:350–61.
[6] Menter T, Haslbauer JD, Nienhold R, et al. Postmortem examination of COVID-19 patients reveals diffuse alveolar damage with severe capillary congestion and variegated findings in lungs and other organs suggesting vascular dysfunction. Histopathology 2020;77:198–209.
[7] Kaminetsky M, Moore W, Fansiwala K, et al. Pulmonary embolism on CTPA in COVID-19 patients. Radiol Cardiothorac Imaging 2020;2(4):e200308.
[8] Ventura-Diaz S, Quintana-Perez JV, Gil-Boronat A, et al. A high D-dimer threshold for predicting pulmonary embolism in patients with COVID-19: a retrospective study. Emerg Radiol 2020. doi: 10.1007/s10140-020-01859-1.
[9] Poissy J, Goutay J, Caplan M, et al. Pulmonary embolism in patients with COVID-19. Awareness of an increased prevalence. Circulation 2020;142:184–6.
[10] Lodigiani C, Lapichino G, Carenzo L, et al. Venous and arterial thromboembolic complications in COVID-19 patients admitted to an academic hospital in Milan, Italy. Thromb. Res. 2020;191:9–14.
[11] Poyiadji N, Cormier P, Patel PY, et al. Acute pulmonary embolism and COVID-19. Radiology 2020;297:E335–8.
[12] Cavagna E, Muratore F, Ferrari F. Pulmonary thromboembolism in COVID-19: venous thromboembolism or arterial thrombosis ? Radiol Cardiothorac Imaging 2020;2(4):e200289.
[13] Ackermann M, Verleden SE, Kuehnel M, et al. Pulmonary vascular endothelialitis, thrombosis, and angiogenesis in COVID-19. N Engl J Med 2020;383:120–8.
[14] Varga Z, Flammer AJ, Steiger P, et al. Endothelial cell infection and endotheliitis in COVID-19. Lancet 2020;395:1417–8.
[15] Lang M, Som A, Mendoza DP, et al. Hypoxemia related to COVID-19: vascular and perfusion abnormalities on dual-energy CT. Lancet Infect Dis 2020;12:1365–6.
[16] Lang M, Som A, Carey D, et al. Pulmonary vascular manifestations of COVID-19 pneumonia. Radiol Cardiothorac Imaging 2020;2(3):e200277.
[17] Ridge CA, Desai SR, Jeyin N, et al. Dual-energy CT pulmonary angiography (DECTPA) quantifies vasculopathy in severe COVID-19 pneumonia. Radiol Cardiothorac Imaging 2020;2(5):e200428.
[18] Patel BV, Arachchillage DJ, Ridge CA, et al. Pulmonary angiopathy in severe COVID-19: physiologic, imaging and hematologic observations. Am J Respir Crit Care Med 2020;202:690–9.
[19] Idilman IS, Dizman GT, Duzgun SA, et al. Lung and kidney perfusion deficits diagnosed with dual-energy computed tomography in patients with COVID-19 related microangiopathy. Eur Radiol 2020. doi: 10.1007/s00330-020-07155-3.

[20] Si-Mohamed S, Chebib N, Sigovan M, et al. In vivo demonstration of pulmonary microvascular involvement in COVID-19 using dual-energy computed tomography. Eur Respir J 2020;56:2002608.
[21] Herrmann J, Mori V, Bates JH, Suki B. Modeling lung perfusion abnormalities to explain early COVID-19 hypoxemia. Nat Commun 2020;11:4883.
[22] Dhawan RT, Gopalan D, Howard L. Beyond the clot: perfusion imaging of the pulmonary vasculature after COVID-19. Lancet Respir Med 2020;S2213-2600(20)30407-0.
[23] Gieraerts C, Dangis A, Janssen L, et al. Prognostic value and reproducibility of AI-assisted analysis of lung involvement in COVID-19 on low-dose submillisievert chest CT: sample size implications for clinical trials. Radiol Cardiothorac Imaging 2020;2(5):e200441.
[24] Quanjer PH, Tammeling GJ, Cotes JE, et al. Lung volumes and forced ventilatory flows. report working party standardization of lung function tests, European community for steel and coal. official statement of the European respiratory society. Eur Respir J 1993(Suppl 16):5–40.
[25] Cotes JE, Chinn DJ, Quanjer PH, et al. Standardization of the measurement of transfer factor (diffusing capacity). Eur Respir J 1993;6:41–52.
[26] Chen JY, Qiao K, Liu F, et al. Lung transplantation as therapeutic option in acute respiratory distress syndrome for coronavirus disease 19-related pulmonary fibrosis. Chin Med J 2020;133:1390–11396.
[27] Combet M, Pavot A, Savale L, et al. Rapid onset honeycombing fibrosis in spontaneously breathing patient with COVID-19. Eur Respir J 2020;56:2001808.
[28] Fox SE, Akmatbekov A, Harbert JL, et al. Pulmonary and cardiac pathology in African American patients with COVID-19: an autopsy series from New Orleans. Lancet Respir Med 2020;8:681–6.
[29] Huertas A, Montani D, Savale L, et al. Endothelial cell dysfunction: a major player in SARS-CoV-2 infection (COVID-19)? Eur Respir J 2020;56(1):2001634.
[30] Frija-Masson J, Debray MP, Gilbert M, et al. Functional characteristics of patients with SARS-CoV-2 pneumonia at 30 days post-infection. Eur Respir J 2020;56:2001754.
[31] Smet J, Stylemans D, Hanon S. Clinical status and lung function 10 weeks after severe SARS-CoV-2 infection. Respir Med 2021;176:106276.
[32] Pansini V, Remy-Jardin M, Faivre JB, et al. Assessment of lobar perfusion in smokers according to the presence and severity of emphysema: preliminary experience with dual-energy CT angiography. Eur Radiol 2009;19:2834–43.
[33] Felloni P, Duhamel A, Faivre JB, et al. Regional distribution of pulmonary blood volume with dual-energy computed tomography: results in 42 subjects. Acad Radiol 2017;24:1412–21.